Proceedings of IMECE2006
2006 ASME International Mechanical Engineering Congress and Exposition
November 5-10, 2006, Chicago, Illinois, USA

IMECE2006-15899

CHARACTERIZING SLOT FILM COOLING THROUGH DETAILED EXPERIMENTS

Carlos A. Cruz
University of Maryland, Department of Aerospace Engineering, College Park, MD
cruzcs@mail.umd.edu

Fernando Raffan
University of Maryland Department of Aerospace Engineering, College Park, MD

Christopher Cadou
University of Maryland, Department of Aerospace Engineering, College Park, MD

André W. Marshall
University of Maryland, Department of Aerospace Engineering, College Park, MD

ABSTRACT

With the ever increasing operating temperatures of gas turbine engines, the surface cooling of hot section components remains a primary consideration in propulsion system design. At the same time, numerical tools are being used more extensively for hot-section flow-path design. Recognizing the need for detailed data to help develop and validate these numerical tools, the present study focuses on characterizing near-wall mixing and heat transfer in a canonical 2D slot film cooling configuration. The lack of comprehensive and detailed experimental film cooling data under realistic temperature and blowing ratio conditions has led the authors to develop and implement a unique experimental facility that will allow measuring velocity and temperature profiles as well as surface temperatures and heat transfer at the wall under adiabatic and isothermal conditions. This hot wind tunnel facility provides optical access for Laser Doppler Velocimetry (LDV) near the wall and wall surface temperature distribution with infrared (IR) thermography. In addition to these non-intrusive diagnostics, the gas-phase temperature is measured with a minimally intrusive micro-thermocouple probe with fast response time and high frequency sampling. The performance of selected film cooling effectiveness scaling laws is analyzed. The thermal and momentum mixing of the film described in terms of temperature and velocity profiles and associated statistics. These detailed measurements are hoped to provide guidance and validation for CFD model developers.

Keywords: slot film cooling effectiveness, gas phase temperature, LDV, streamwise velocity profiles

INTRODUCTION

Film cooling is a technique widely used to protect engine components from the extreme thermal loads generated by the combustion process. Such components include combustor walls, turbine blades and in some cases exhaust nozzles. Injected as liquid or a gas the coolant film is injected through a combination of holes and slots. It is critical to understand the complex dynamics governing the mixing of the film and consequently the cooling effectiveness of the film. Although significant progress has been made in Computational Fluid Dynamics (CFD), especially with Large-Eddy Simulations (LES), the computational cost associated to engineering type flows remains prohibitive. Modeling approaches based on wall models specifically developed for film cooling could improve drastically the computational cost of those simulations and capture the important physics at the wall. For such modeling initiatives detailed gas phase measurements of temperature and velocity are needed to provide test cases for model development and validation.

Previous Work

During early developments of gas turbine engines, film cooling has been studied with great interest. Among those early studies, Wieghardt [1] analyzed the effect of injection of warm air through a two-dimensional slot as a de-icing device. At different injection angles and blowing ratios he studied the entrainment of the film by the mainstream. Wieghardt derived a similarity expression for the gas phase temperature based on the local adiabatic wall temperature and thermal boundary layer thickness. Following this study several experimental works proposed expressions for the film cooling effectiveness [2, 3]. Following these developments Stollery and El-Ehwany [4] developed an expression for the film cooling effectiveness based on enthalpy and mentioned the experimental scatter in Hartnett and al. [3] is mainly due to different slot Reynolds numbers. This parameter is hence

identified as characteristic of the initial state of turbulence. Since the film cooling effectiveness correlations are based on fully developed boundary layer and constant fluid property assumptions they cannot be applied near the slot where these assumptions do not hold. In an attempt to solve this problem Ballal and Lefebvre [5] used previous analysis [4, 6] and direct measurements of the skin friction coefficient near the slot to derive an expression for the effectiveness in this region. The resulting semi-empirical correlation showed good agreement with experimental data within 5%. At high blowing ratios, Ballal and Lefebvre [5] developed a correlation for the effectiveness based on wall jet theory. The reader is referred to Goldstein [7] for a comprehensive review of early film cooling effectiveness correlations.

The adiabatic film cooling effectiveness being a measure of the film mixing, Marek and Tacina [8] derived a correlation based on the axial turbulence intensity of the mainstream and an empirical mixing coefficient. They noticed that a constant mixing coefficient along the plate leads to ± 30 % agreement with experimental data. Following this study, Simon [9] performed a similar wall jet analysis and considered the wall normal turbulence intensities of both mainstream and coolant flows to evaluate a mixing coefficient varying along the plate. This film cooling model requires an iteration procedure to calculate the film cooling effectiveness and agrees within ± 4 % of Marek and Tacina's experimental data. One should note however that the constants in Simon model were obtained using Marek and Tacina data.

Film Cooling Prediction

The adiabatic film cooling effectiveness is based on the adiabatic wall temperature concept and is given by

$$\eta = (T_\infty - T_{aw})/(T_\infty - T_c) \quad (1)$$

where T_{aw}, T_c and T_∞ are the temperature of the adiabatic wall, the cooling air and the hot mainstream, respectively. The effectiveness is equal to unity at the exit of the slot and then decreases to zero far downstream where the film has mixed with the mainstream. As mentioned by Goldstein [7], the effectiveness depends on several flow parameters such as the temperature ratio T_∞/T_c, the velocity ratio U_c/U_∞, the blowing ratio $m = (\rho U)_c / (\rho U)_\infty$, and the slot Reynolds number $\mathrm{Re}_s = (U_c\, s)/\nu$ base on the slot exit height s and velocity U_c. Using the appropriate correlation [10] for the adiabatic film cooling effectiveness, the adiabatic wall temperature is readily obtained along the wall. The reference temperature is then used to calculate the convective heat flux at the wall. The convective heat flux can be expressed in terms film cooling effectiveness using

$$q''_{conv} = h_x(T_\infty - \eta(T_\infty - T_c) - T_w) \quad (2)$$

Equation where h_x is the local convective heat transfer coefficient, which can be determined by using the appropriate Nusselt number correlation depending the blowing ratio [10]. The accuracy of the heat transfer prediction is mainly limited by the accuracy of the heat transfer coefficient and cooling effectiveness correlations. Using a different film cooling model for the effectiveness, such as the one developed by Simon [9], can lead to a more accurate prediction of the heat transfer problem at a film cooled wall. Although this approach rests on the use of scaling laws and strong simplifying assumptions it allows an analysis of the film cooling requirements for engineering applications.

In recent years advanced CFD models such as LES have gained more interest for engineering applications, due in part to increased computational power. Several authors studied numerical simulations of film cooling through a two-dimensional slot. Among those early studies Zhou, Salcudean and Gartshore [11] modeled the turbulence using a k-ε model with a near-wall low-Reynolds-number k model and also a k-ε model with a wall function. For blowing ratios less 0.4 their results showed good agreement with experimental data. Jansson, Davidson and Olsson [12] modeled film cooling through a slot by a standard k-ε model and an algebraic stress model. Their results showed good agreement for velocity profiles. However the comparison in terms of temperature profiles presented significant differences due to measurement issues and to the modeling errors especially in the diffusive terms of the temperature transport equation. More recently a Detached Eddy Simulation (DES) was performed on a film cooling configuration over a flat plate with film injection through discrete holes [13]. DES is a promising hybrid modeling tool using RANS formulation near the wall and a LES formulation further away. In this study the authors mentioned a strong anisotropic mixing not well captured by RANS and limitations of the simulation due to symmetry boundary conditions in the computational domain. Even if the cost associated with this simulation is less than that of a DNS, it remains too expensive for engineering applications. An alternative to this problem would be to use a coarse grid and the appropriate sub-grid scale model for the physics of the mixing and heat transfer at a film-cooled wall.

Previous experimental studies have focused significantly on the wall temperature and corresponding adiabatic film cooling effectiveness. However as recent numerical studies pointed out, it appears that near wall temperature profiles and the corresponding wall heat flux are difficult to predict accurately [12]. High quality gas phase, velocity profiles and wall temperature measurements under realistic flow conditions (blowing ratio, temperature ratio, slot Reynolds number, turbulence intensity) are needed to help develop and validate emerging CFD near-wall mixing and heat transfer models for film cooling application.

Objectives

The main objective of this study is to provide a characterization of film cooling through two-dimensional slot with detailed surface and gas phase temperature and streamwise velocity measurements. The experimental facility and diagnostics associated with those challenging measurements will be introduced. The performance of existing cooling effectiveness scaling laws will be explored

and compared to current experimental data for blowing ratios consistent with engineering applications. In addition, the gas phase temperature measurements and the detailed analysis of the associated statistics will provide a characterization of the thermal mixing of the film and near-wall transport. Finally the streamwise velocity measurements in the film and the mixing region will provide additional information regarding the mixing of the film for a wall jet configuration. Those detailed measurements are hoped to serve model developers in validating existing or future CFD models.

EXPERIMENTAL FACILITY AND DIAGNOSTICS

A hot wind tunnel facility was specially designed for the study of film cooling under conditions relevant to gas turbine engines and rocket thrust chambers. In this section the specific components of the facility are described, and the diagnostics are presented along with the data post-processing techniques.

Hot Wind Tunnel Facility Characteristics

As portrayed in Figure 1, this wind tunnel is an open circuit system that includes a centrifugal fan, a methane burner, a settling chamber with flow control devices (ceramic saddles, screens, etc.), a two-dimensional convergent with a contraction ratio of 6:1 and a test section. Downstream of the test section an optimized two-dimensional diffuser reduces pressure losses. Exhaust gases are vented through a duct. To create the cooling film, a high capacity compressor delivers air into a plenum, which is subsequently injected into the test section through a louvered slot, thus creating a tangential film. The use of hot vitiated air in the mainstream provides a realistic experimental configuration for investigating heat transfer in gas turbine engines and rocket thrust chambers. Operating conditions span those encountered in rocket thrust chambers, as well as those found in gas turbines, with velocity ratios U_c/U_∞ up to 3, absolute temperature ratios T_∞/T_c up to 2, and blowing ratios $\rho_c U_c/\rho_\infty U_\infty$ in excess of 5. Although the experimental slot injection Reynolds numbers Re_s, are significantly smaller than those found in propulsion applications, they are still in the turbulent regime, ranging from 2000 to 6000.

The wind tunnel uses a centrifugal fan driven by a 3-phase electric motor. A frequency controller allows for variation of the fan rotation speed. Downstream of the fan, a methane inline burner is mounted inside the flame tube to heat the air. Flow detachment and pressure losses at high speeds are minimized through the use of turning vanes in the elbow. In the settling chamber, several devices are used for flow control. First the flow is thermally mixed and homogenized as it passes through a 10-cm-long obstruction made of randomly packed ceramic saddles. This thermal buffer also filters flow inhomogeneities generated by the burner. Then, large scale wall normal (y) and spanwise (z) turbulent structures are damped as the flow passes through a welded stainless steel honeycomb with characteristic cell diameter of 3.17 mm and length of 15.87 mm [14]. Finally, a fine mesh screen is placed before the inlet of the contraction. The stainless steel 2D convergent section with a contraction ratio of 6:1 is mounted downstream of the settling chamber.

The test section is made out of a stainless steel flanged channel 200 by 50 mm cross-section and 500 mm-long directly connected to the convergent. The louvered slot is mounted to the test plate, which is made of UDEL®, a high temperature thermoplastic. This material was chosen for its transparency (80% of visible light), which helps to reduce the optical noise encountered in diagnostics like LDV and PIV.

The slot geometrical characteristics can easily be modified. For the present paper, the slot thickness s is set to 2.1 mm, the louver is 0.76 mm thick and 50 mm long as represented in Figure 2. The film flow is injected through discrete holes 3.17 mm in diameter separated by 6.35 mm. These jets impinge on the louver and coalesce to create a film at the exit of the slot. For additional details on the components of the facility the reader is referred to Cruz and Marshall [15].

Diagnostics

The test facility is equipped with instruments to characterize the mainstream and the cooling film inlet conditions (i.e. velocity and temperature), allowing for the control of velocity ratios, temperature ratios and, ultimately,

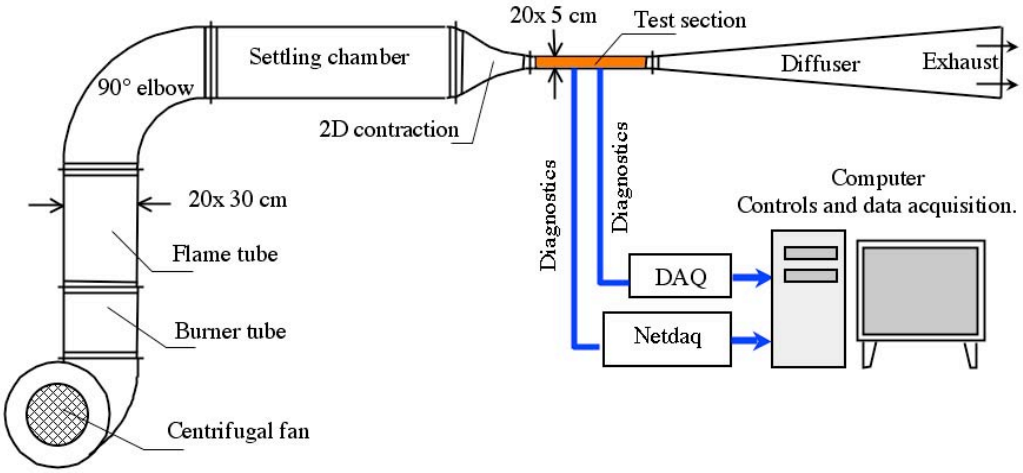

Figure 1. Hot Wind Tunnels, layout of the facility components and diagnostics. (From [18])

blowing ratios. Once a blowing ratio is set and the thermal steady-state of the test plate is reached, temperature and velocity profiles are obtained at select locations downstream of the slot. The test section geometry and diagnostics are presented in Figure 2.

Operating and Inlet Conditions

The mainstream inlet conditions are measured with a small size Pitot tube equipped with a micro-thermocouple. It includes static and total pressure taps made of 1/16" OD stainless steel tubes and a 50µm-diameter type K thermocouple insulated in a ceramic tube. Analog temperature and pressure difference are recorded with a Labview DAQ data acquisition board, sampled at 1 kHz and processed to calculate the velocity and the temperature.

The cooling air temperature is measured near the exit of the slot with a 50-µm-wire diameter type K thermocouple, insulated in a ceramic tube. The small probe is inserted through a hole on the test plate and the junction measures T_c the cooling flow temperature between the louver and the test plate. The average velocity at the exit of the slot is evaluated by mass flow conservation.

Temperature Measurements

Temperature readings are obtained through surface thermocouples to measure the adiabatic wall temperature and a micro-thermocouple probe to measure the gas phase temperature profiles and access mixing and turbulence scale information. Surface thermocouples on the casing allow corrections for radiation effects on the wall. The wall surface temperatures are measured with 12 type K surface-mounted thermocouples fixed at different x-locations downstream of the slot. They are attached to the external surface of the test plate to avoid perturbation of the flow. The external surface of the test plate is insulated with *Kaowool* board from Thermal Ceramics. Preliminary experiments showed the external surface of the insulation to be less than 1ºC above the ambient temperature. Using the low thermal conductivity of the insulation (0.06 $W.m^{-1}.K^{-1}$) and the temperature gradient across the 1-inch thick board, the heat losses are estimated to be negligible. The wall temperature measurements were corrected for thermal radiation from the casing using the measured casing temperatures and a radiosity approach [16].

Gas temperatures are measured with a micro-thermocouple probe. A 13µm-wire-diameter type K thermocouple is threaded through a double holed ceramic insulation inside a stainless steel tube. The bead extends 2 mm outside the ceramic and the stainless tube to avoid flow disturbances at the measurement location. Given Shaddix's recommendations [17], this distance is also sufficiently long to neglect thermal conduction from contaminating the temperature measurements even under the largest gas phase temperature gradients measured. The probe is inserted through several port holes in the casing to measure temperature profiles at selected x-positions downstream of the slot exit and traversed from the wall with a 10µm-precision traverse. Data were recorded at a 20 kHz sampling frequency during 30 seconds. The time constant of the thermocouple probe was directly obtained by

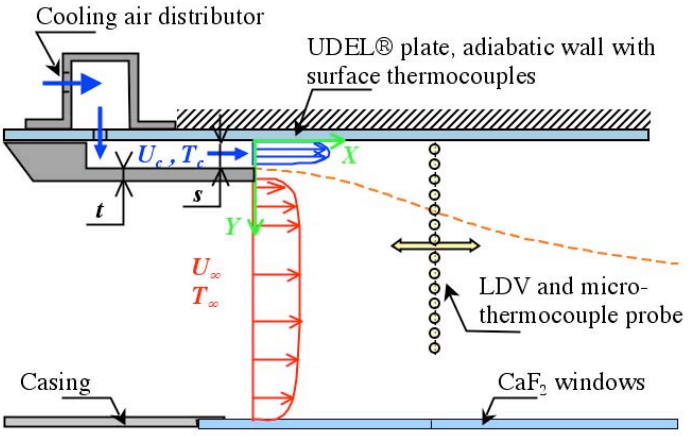

Figure 2. Schematic of the tests section and diagnostics

measuring in the test section the cooling cycle of the probe resulting from an electrically heated cycle. Typical values for the time constant are in the range 1.6 to 2.2 ms. The response time of the probe was used to correct for its thermal inertia and hence recover the actual fluctuations in the temperature signal [18].

Laser Doppler Velocimetry

Velocity measurements are performed in cold flow for the same velocity ratio used during the hot flow temperature measurements. A single component TSI Laser Doppler Velocimetry system, operating in backscatter mode is used to measure velocities. Using two fluidized bed seeders, built according to the suggestions found in [19], TiO_2 particles are introduced in the mainstream and in the slot. As with any scattered light based technique, the particles must be large enough for the collector to detect the scattered light. However, the particles need to be small in order to faithfully follow the flow. A particle size on the order of 1-2 µm proved to be a good compromise, as presented by Melling [20].

The seeders allow for a continuous delivery of particles at the injection point, and the seeding density can be actively controlled during the experiment. The mainstream is seeded directly at the fan, to enhance seeding homogeneity in the flow, while the film is seeded upstream of the plenum. Flowmeters and pressure gauges are used to obtain the seeded film velocity, based on massflow calculations.

The LDV probe is mounted on a traverse with 10-µm-displacement precision. The probe can be rotated on the z-axis to measure the streamwise or the wall-normal component of the velocity. A typical data rate of 80 Hz is obtained at each measurement point, and statistics are taken over 500 samples. The size of the sample was determined sufficient to obtain repeatable statistics. Three distinct streamwise profiles are obtained, each one at a different location downstream of the slot exit. For more information on the LDV system, the flow analyzer and the data acquisition, the reader is referred to Yao [21].

RESULT ANALYSIS

The operating conditions for the different tests considered here are presented in Table 1. These tests cover a large range of: blowing ratios from 0.66 to 2.29, temperature ratios from 1.35 to 1.62 and slot Reynolds numbers from 1850 to 5170.

Table 1. Test Operating Conditions

Test	T_∞, K	T_c, K	U_∞, m/s	U_c, m/s	T_∞/T_c	m	Re_s
1	428	318	24.4	12.0	1.35	0.66	1850
2	515	331	25.6	12.5	1.56	0.76	1790
3	515	319	26.7	21.2	1.62	1.28	3240
4	413	306	23.0	22.0	1.35	1.29	3600
5	429	309	19.9	28.8	1.39	2.00	4660
6	431	306	20.0	31.5	1.41	2.22	5170
7	429	306	17.5	28.6	1.40	2.29	4700

First, the performance of simple correlations for the adiabatic film cooling effectiveness will be examined. It will be followed by an analysis of the gas phase temperature measurements and statistics for Test 7. This analysis will provide insight into the thermal mixing of the film and mainstream. The momentum mixing of the film will also be studied through velocity measurements and statistics.

Adiabatic Film Cooling Effectiveness

The adiabatic film cooling effectiveness, as introduced by Eq. (1), is an important concept for predicting the heat flux at a film-cooled wall using simple correlations. The analysis of the performance of those correlations is critical. In this study we considered two effectiveness scaling laws: Lefebvre's correlation based on turbulent boundary layer which has been reported to perform well [10], and Simon's model, based on a wall jet mixing approach. To the authors knowledge this model has not been used in published literature. The performance of this model is compared to present experimental data.

The first correlation, from Lefebvre [10], is based on turbulent boundary layer analysis and is valid for blowing ratios in the range 0.5 to 1.3. The effectiveness is a function of the position x, the slot height s, the blowing ratio m, the slot Reynolds number Re_s and the ratio of dynamic viscosities between the film and mainstream

$$\eta = 0.6\left(\frac{x}{m\,s}\right)^{-0.3}\left(\mathrm{Re}_s\,\frac{m\,\mu_c}{\mu_\infty}\right)^{0.15} \qquad (3)$$

The performance of this correlation is examined in Figure 3 and compared to experimental data from Test 1 to 4, for blowing ratios in the range 0.66 to 1.29. It can be observed that this correlation tends to underpredict the film effectiveness in the near slot region. In the far field region (x/s > 80) the correlation tends to provide a reasonable estimate of the effectiveness. However one can notice that for Test 3 the far field effectiveness is overpredicted while this is not the case for Test 4 that has a similar blowing ratio. This phenomenon can be related to the difference in temperature ratio between those two Tests, Test 3 having a larger temperature ratio than Test 4. Experimental data show the temperature ratio effect is not significantly taken into account by the correlation. This prediction can even lead to wrong trends in the far field when comparing Test 1 and 2. The correlation predicts a larger effectiveness for Test 2 (due to a larger blowing ratio) while experimental data show that Test 1

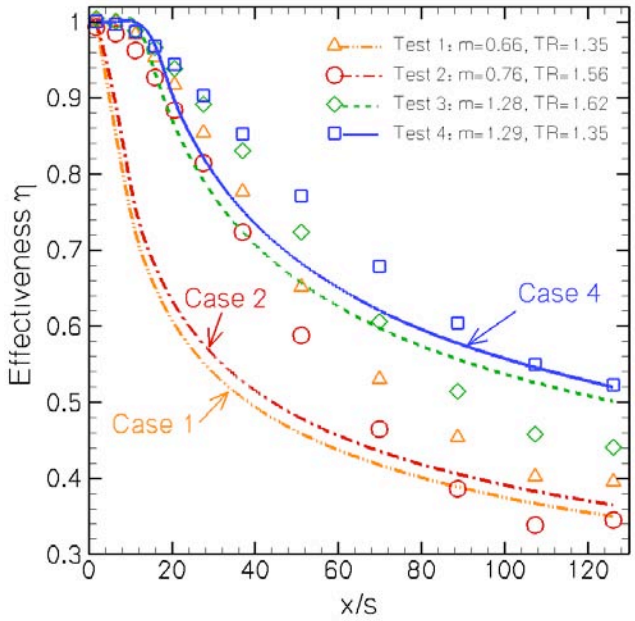

Figure 3. Film cooling effectiveness for low blowing ratios, comparison of experimental data from Test 1 through 4 to the prediction using Lefebvre correlation based on turbulent boundary layer analysis [10]

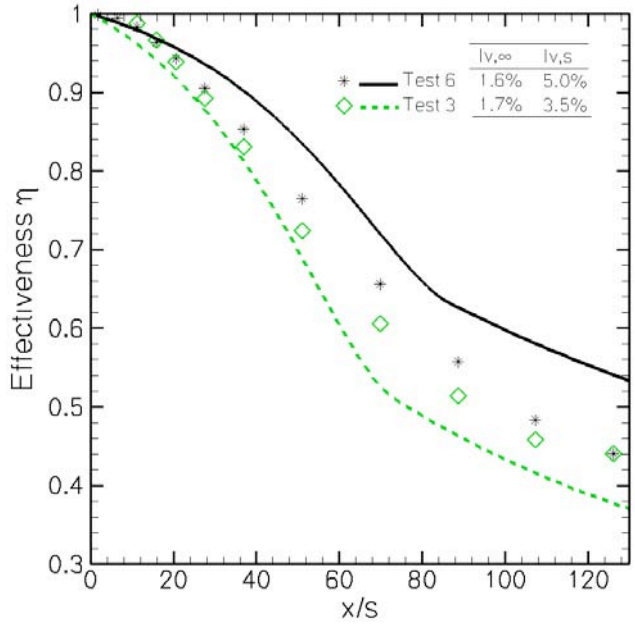

Figure 4. Film cooling effectiveness, comparison of experimental data from Test 3 and 6 to the prediction using Simon's model [9]

has a larger effectiveness. In the transition region, between near field and far field, the effectiveness is significantly underpredicted for most the cases presented in Figure 1. For Test 1 and 2 particularly, the prediction of the effectiveness can be underestimate by more than 10% for *x/s* in the range 10 to 60. For higher blowing ratios (Test 3 and 4) this error is less pronounced.

The second scaling law examined here was developed by Simon [9] and is based on a wall jet analysis that distinguishes an initial region near the slot exit and a subsequent fully developed region further downstream. The mixing between the film and the mainstream is calculated based on the wall normal turbulence intensities of the film and the mainstream, $I_{v,s}$ and $I_{v,\infty}$ respectively. The iterative calculation procedure to obtain the cooling effectiveness is presented by Simon in detail. Figure 4 presents the comparison of the prediction of Simon's scaling law for Test 3 and 6 with the experimental data. In contrast to Lefebvre's correlation, the prediction of the film cooling effectiveness is in excellent agreement in the near slot region. For both Tests the trends are well captured, in particular the inflection point and the transition from the initial region to the fully developed region. One can notice however that for Test 6 the scaling law consistently tends to overpredict the effectiveness and particularly in the far field region. This is consistent with Simon findings for turbulence intensities lower than 8 %. However this cannot explain the fact that the scaling law slightly underpredicts the effectiveness for Test 3. This has not been observed by Simon and could be related to high temperature ratio effect mentioned above. It is also worth noting that Simon's model was only validated for *x/s* less than 30, but this scaling law provides a reasonable estimate of the effectiveness even in the far stream as Figure 4 demonstrates.

Film Thermal Mixing

The gas phase temperatures are measured with a micro-thermocouple probe. The raw temperature data are compensated for the thermal inertia of the probe based on its time constant. Temperature statistics are performed on the instantaneous realization samples.

Figure 5 shows the mean temperature profiles non-dimensionalized by $(T_\infty\text{-}T)/(T_\infty\text{-}T_c)$ obtained for Test 7. Data are presented at four locations downstream of the slot exit defined by *x/s* equal to 1.8, 16, 70 and 107. The first measurement from the wall is approximately one probe diameter from the wall, i.e. 13 µm. This closest point from the wall agrees very well with adiabatic wall temperature measurements. Near the wall the temperature gradient is virtually zero, which indicates a good adiabatic wall conditions. The first profile (*x/s* =1.8) has a very sharp gradient from the coolant temperature (i.e. dimensionless temperature of unity) to the hot mainstream (i.e. dimensionless temperature equal to zero). As we go further away from the slot exit, the temperature profiles evolve and the gradients at the interface between the two streams become weaker. The interface and mixing region itself grows with the distance *x/s* and allows for the penetration of hot gases closer to wall. This mixing is responsible for the loss in cooling effectiveness. Consequently it appears critical to understand the physics involved in this mixing.

The thermal mixing of the film and mainstream can be further analyzed by considering the RMS of the same gas phase temperature shown in Figure 6. In this figure the RMS of temperature is non-dimensionalized by the local mean temperature. Near the exit of the slot (i.e. *x/s* = 1.8) the RMS is large at the interface of the two streams. The peak occurs at

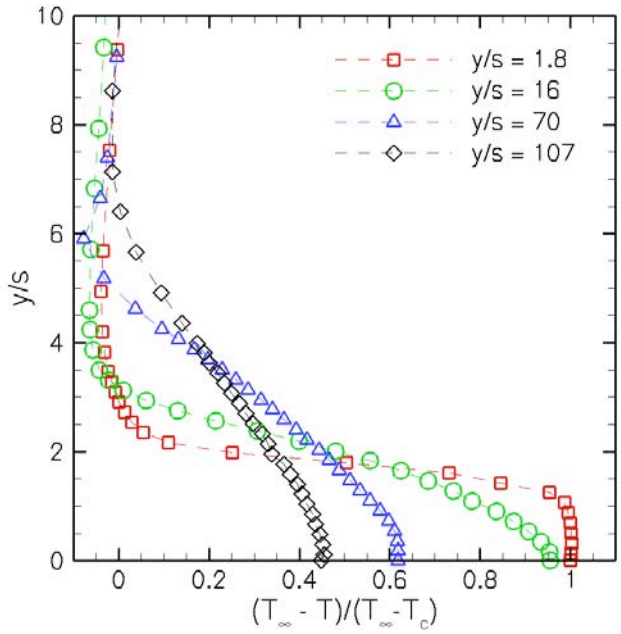

Figure 5. Dimensionless mean temperature profiles, $(T_\infty\text{-}T)/(T_\infty\text{-}T_c)$, at four *x/s* locations downstream of the slot, from Test 7, *m* = 2.29.

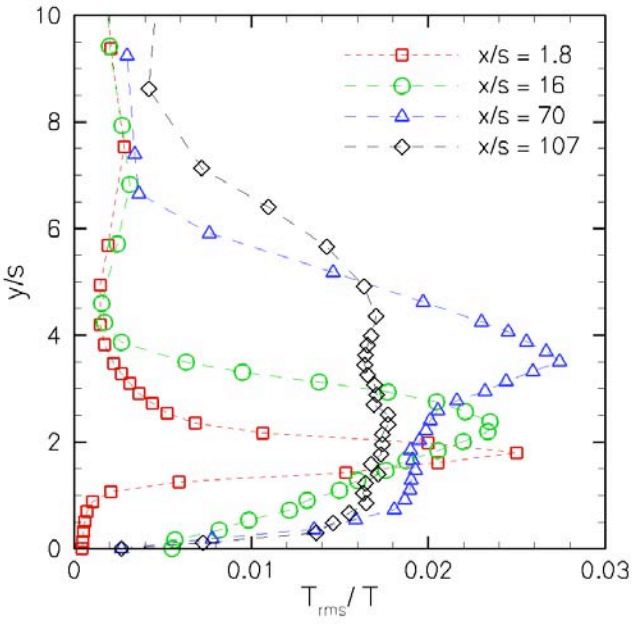

Figure 6. Dimensionless gas temperature RMS profiles, T_{rms}/T, at four *x/s* locations downstream of the slot, from Test 7, *m* = 2.29.

about 2 slot heights from the wall. The RMS levels in the slot and the mainstream remain low indicating well mixed inlet conditions. The large gradients of RMS near the peak suggest a sharp mixing interface due to the strong shear. At the next location downstream, the mixing interface grows and reaches closer to the wall. In particular the peak RMS location is further away from the wall at *y/s* about 2.5. At *x/s* equal to 70 the RMS profile shows the intense mixing has propagated closer to the wall and the peak RMS now occurs further away from the wall. Finally at *x/s* equal to 107 the RMS levels become flatter across the wall jet and the peak is not easily discernable. This indicates intense mixing is taking place from the wall to the edge of the mainstream.

Film Momentum Mixing

The wind tunnel was operated in a cold flow configuration, for a velocity ratio corresponding to that of Test 7 in Table 1. The mainstream mean velocity U_∞ was measured with the Pitot tube, with a value of 10 m/s. Based on massflow calculations, the jet injection velocity U_{jet} was 15.75 m/s. Once these values were set, the 3 streamwise profiles were obtained with the LDV probe. Those near wall measurements are very challenging due to the small size of the slot and the wall jet velocity magnitudes considered. Due to a weak LDV signal near the wall, the seeding concentration was increased in the film. Figure 7 shows the streamwise mean velocity profiles normalized by the jet velocity, U_{jet}, at 3 distinct *x* locations, downstream of the slot exit. Figure 8 shows the turbulence intensities defined as U_{rms}/U, that is, the standard deviation of the streamwise velocity divided by the local mean velocity. For both figures the wall normal distance is normalized by the slot height, *s*.

Near the slot, at *x/s* = 2.3, the wall jet is clearly identified. The peak jet velocity is observed halfway through the slot height. The velocity deficit observed for *y/s* in the range 1 to 2.5 is induced by the louver thickness. Two turbulence intensity peaks are observed. The first one close to the wall is due to wall turbulence effects. The turbulence intensity then decays and another peak is found near the slot height at the interface between the film and the mainstream. This peak suggests intense mixing due to the presence of the shear layer.

At the next downstream location, namely *x/s* = 21, the wall jet growth is observed. Due to the shear and turbulent mixing the mean velocity profile adapts and overcomes the velocity deficit due to the louver lip. The size of the wall jet grows, as the maximum velocity point is located further away from the wall. Although the measurements near the wall and in the freestream appear reasonable, the measurements in the mixing region contain errors, as pictured in Figure 7. These errors are due to velocity bias and seeding concentration bias [22]. The natural bias towards higher velocities is dues to a higher representation of fast moving particles. The mean velocity in this plot was not corrected for this phenomenon. The seeding concentration bias is due to a higher particle concentration in the film than in the freestream. This leads to a significant bias towards high velocity in the mixing region. Once again, two turbulence intensity peaks are observed, which is consistent with the two-layer description of a wall jet made by Lauder and Rodi [23]. They mainly describe a wall layer where the flow behaves like a boundary layer and a free shear flow in the outer region. The wall effects are still present, while the shear layer effects can be observed further from the wall as in the previous x/s location. This clearly indicates the growth of the jet, and verifies that mixing is taking place between the streams.

At *x/s* = 118, the flow is very homogenous. A flat mean velocity profile is observed, indicating that the streams are

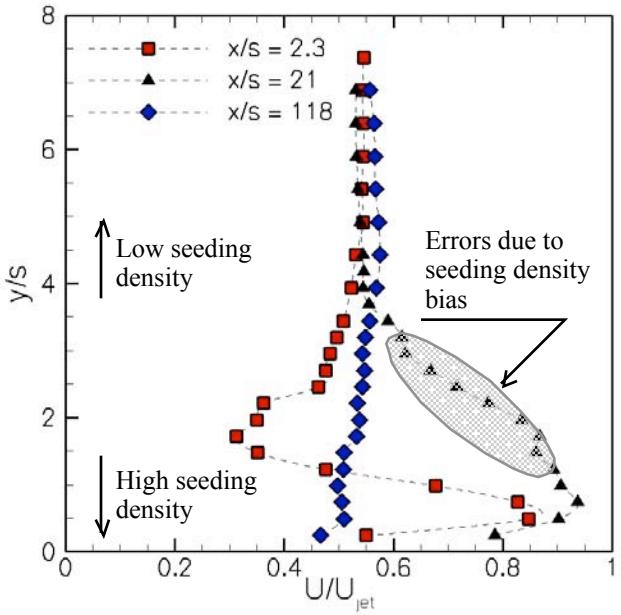

Figure 7. Streamwise velocity profiles non-dimensionalized by the jet velocity U_{jet} = 15.75 m/s, for U_∞/U_{jet} = 0.55.

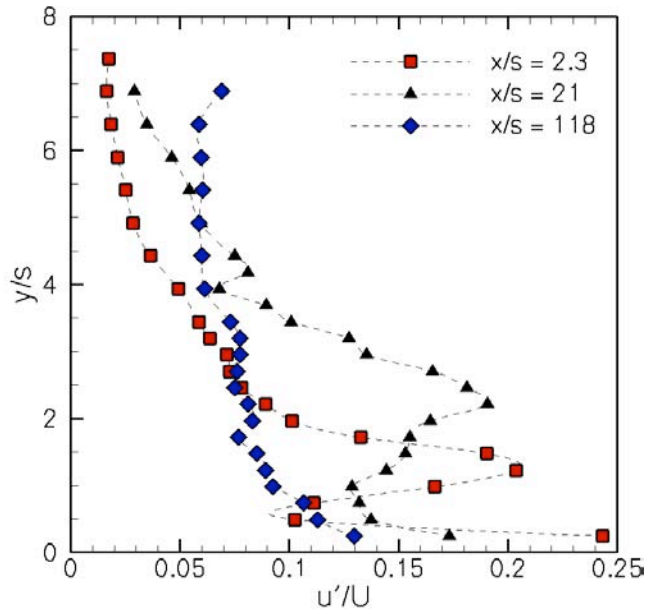

Figure 8. Streamwise turbulence intensity profiles u'/U for U_∞/U_{jet} = 0.55.

well mixed and behave as a single stream. The turbulence intensity profile at this streamwise location verifies this, as the only significant peak is observed near the wall.

Some remarks can be drawn when comparing the results for momentum mixing to those for thermal mixing. Initially the mixing is due to the large velocity and temperature gradients between both streams, as indicated by the RMS profiles. Further downstream both velocity and temperature gradients are decreased due to intense turbulent mixing. At the furthest streamwise location, the velocity profile indicates a well-mixed state. However the temperature profile indicates that the temperature near the wall is still cooler than the mainstream, emphasizing the film cooling effectiveness has not vanished. Intense fluctuations of temperature and velocity are associated with large gradients. Due to the adiabatic condition at the wall, the temperature gradients are small and lead to reduced fluctuations of temperature near the wall. However, the no-slip conditions at the wall leads to large gradients and intense near wall momentum mixing as characterized in the turbulence intensity profiles. This emphasizes the different nature of thermal and momentum mixing near the wall.

CONCLUSION

Measurements of the adiabatic effectiveness were performed in a hot wind tunnel under well-characterized inlet conditions. Experimental data were obtained over a range of operating conditions and compared to previously developed correlations for the effectiveness based on boundary layer or wall-jet theories. The comparison showed that for low to moderate blowing ratios the selected boundary-layer-based correlation consistently underpredicts effectiveness in the midfield region. In addition, this comparison revealed that the correlation is not sensitive enough to temperature ratio. By considering the inlet turbulence intensities, Simon's model showed better prediction of the data both in the near field and midfield regions. It also performed well in the farfield, region where it has not been previously validated due to lack of experimental data.

Detailed gas phase temperatures were measured under excellent adiabatic wall conditions. The streamwise velocity profiles were obtained at the same velocity ratio under cold flow conditions. These challenging measurements provided insight into the complex dynamics involved in the thermal and momentum mixing between the film and the mainstream, in particular the growth the turbulent mixing region and growth of the wall jet. The RMS profiles of temperature and streamwise velocity indicate similarities. However the near wall behavior seems to suggest more intense fluctuations in terms of momentum than in terms of temperature. This different near wall mixing behavior is due to small temperature gradients imposed by the adiabatic wall condition, whereas velocity gradients are large near the wall. These detailed measurements with well-defined inlet conditions provide information to support CFD model development and validation in a way not possible from existing scaling laws.

ACKNOWLEDGMENTS

This work has been sponsored by the Space Vehicles Technology Institute, grant NCC3-989, one of the NASA University Institutes, with joint sponsorship from the Department of Defense. Appreciation is expressed to Claudia Meyer of the NASA Glenn Research Center, program manager of the University Institute activity, and to Dr. John Schmisseur and Dr. Walter Jones of the Air Force Office of Scientific Research.

REFERENCES

[1] Wieghardt, K. "Hot Air Discharge for De-Icing", AAF Trans. No. F-TS-919-RE, *Air Material Command*, Dec. 1946.

[2] Tribus M. and Klein J., "Forced Convection From Non-Isothermal Surfaces", Heat Transfer, a Symposium, University of Michigan Press, Ann Arbor, Mich.., 1953.

[3] Hartnett, J. P., Birkebak, R. C. and Eckert, E. R. G., "Velocity distributions, Temperature Distributions, Effectiveness and Heat Transfer for Air Injected Through a Tangential Slot Into a Turbulent Boundary layer", *Journal of Heat Transfer*, August 1961, pp. 293-306.

[4] Stollery, J. L. and El-Ehwany, A. A. M., "A Note on the Use of Boundary-Layer Model for Correlating Film Cooling Data", *Int. J. of Heat and Mass Transfer*, vol.8, no.1, 1965, pp. 55-65.

[5] Ballal, D. R., and Lefebvre, A. H., "Film Cooling Effectiveness in the Near Slot Region", Journal of Heat Transfer, May 1973, pp. 165-166.

[6] Burns, W. K., and Stollery, J. L., "The Influence Foreign Gas Injection and Slot Geometry on Film Cooling Effectiveness", *International Journal of Heat and Mass Transfer*, vol. 12, 1969, pp. 935-951.

[7] Goldstein, R. J., Film Cooling, *in Advances in Heat Transfer*, vol.7, Academic Press, New York, 1971, pp. 321-378.

[8] Marek, C. J., and Tacina, R. R., "Effect of Free-Stream Turbulence on Film Cooling", NASA TN D-7958, 1975.

[9] Simon, F. F., "Jet Model for Slot Film Cooling With Effect of Free-Stream and Coolant Turbulence", NASA TP 2655, October 1986.

[10] Lefebvre, A. H., *Gas Turbine Combustion,* Taylor & Francis, 1983.

[11] Zhou, J. M., Salcudean, M. and Gartshore, I. S., "A Numerical Computation of Film Cooling Effectiveness", *Near-Wall Turbulent Flows*, Elsevier Science Publishers, 1993, pp. 377-386,

[12] Jansson, L. S., Davidson, L., and Olsson, E., "Calculation of Steady and Unsteady Flows in a Film-Cooling Arrangement Using a Two-Layer Algebraic Stress Model", *Numerical Heat Transfer*, Part A, vol. 25, 1994, pp. 237-258.

[13] Roy, S., Kapadia, S. and Heidmann J. D., "Film Cooling Analysis Using DES Turbulence Model", ASME Turbo Expo, paper GT 2003-38140, June 2003.

[14] Mehta, R. D. and Bradshaw, P., "Design Rules for Small Low Speed Wind Tunnels", Technical Note Reprinted from *The Aeronautical Journal of the Royal Aeronautical Society*, November 1979.

[15] Cruz, C. A., and Marshall, A. W., "Surface and Gas Phase Temperatures Near a Film Cooled Wall", AIAA-2004-3654, 2004.

[16] Modest, M. F., *Radiative Heat Transfer*, McGraw-Hill, 1993, pp. 200-217.

[17] Shaddix, C. R. "Practical Aspects of Correcting Thermocouple Measurements for Radiation Loss", Western State Section/The Combustion Institute, WSS/CI 98F-14, 1998.

[18] Cruz, C. A., and Marshall, A. W., "Surface and Gas Measurements Along a Film Cooled Wall", *Journal of*

Thermophysics and Heat Transfer, Accepted for publication July 2006.
[19] Yerushalmi, J., "High Velocity Fluidized Beds", in Geldart D. ed. *Gas Fluidization Technology*, John Wiley & Sons, pp. 155-196, 1986.
[20] Melling, A., "Tracer Particles and Seeding for Particle Image Velocimetry", Measurement Science and Technology, vol. 8, # 12, pp. 1406-1416, 1997.
[21] Yao, X., "Characterization of Fire Induced Flow Transport Along Ceilings Using Salt-Water Modeling", PhD Dissertation, University of Maryland, 2006.
[22] Durst, F., Melling, A., and Whitelaw, J. H., *Principles and Practice of Laser-Doppler Anemometry*, Academic Press, 2nd Edition, pp. 270-279, 1981.
[23] Lauder, B. E. and Rodi W., "The Turbulent Wall Jet – Measurement and Modeling", *Annual Review of Fluid Mechanics*, vol. 15, 1983, pp. 429-459.